Thermodynamically consistent equilibrium properties of normal-liquid ^{3}He

M. Kollar* and D. Vollhardt
Theoretische Physik III, Elektronische Korrelationen und Magnetismus, Institut für Physik, Universität Augsburg, D-86135 Augsburg, Germany
(Received 1 June 1999)

The high-precision data for the specific heat $C_V(T,V)$ of normal-liquid ^{3}He obtained by Greywall, taken together with the molar volume $V(T_0,P)$ at one temperature T_0, are shown to contain the complete thermodynamic information about this phase in zero magnetic field. This enables us to calculate the T and P dependence of all equilibrium properties of normal-liquid ^{3}He in a thermodynamically consistent way for a wide range of parameters. The results for the entropy $S(T,P)$, specific heat at constant pressure $C_P(T,P)$, molar volume $V(T,P)$, compressibility $\kappa(T,P)$, and thermal expansion coefficient $\alpha(T,P)$ are collected in the form of figures and tables. This provides the first complete set of thermodynamically consistent values of the equilibrium quantities of normal-liquid ^{3}He. We find, for example, that $\alpha(T,P)$ has a surprisingly intricate pressure dependence at low temperatures, and that the curves $\alpha(T,P)$ vs T do not cross at one single temperature for all pressures, in contrast to the curves presented in the comprehensive survey of helium by Wilks.

I. INTRODUCTION

Liquid ^{3}He is an exceptional system: at sufficiently low temperatures its normal phase is the prototype of a Landau Fermi liquid,[1,2] while the superfluid phases, appearing at even lower temperatures, present examples of anisotropic BCS-type superfluids.[3,4] Therefore liquid ^{3}He has been investigated systematically and in considerable detail at temperatures T both below the critical temperature T_c in the superfluid state ($T<T_c=0.0026$ K)[5,3] and in the Fermi liquid regime ($T_c<T\lesssim 0.16$ K).[6,7] At higher temperatures the dependence of the molar volume V, entropy S, thermal expansion coefficient α, and specific heat C_P on pressure P had already been measured earlier by different groups.[8–13] Their values are summarized in figures, as well as tables in the appendixes, in the comprehensive book by Wilks.[6] Later measurements of some of these quantities were made, for example, by Grilly[14] and by Abraham and Osborne.[15] Subsequently, high-precision measurements of the specific heat at constant volume, $C_V(T,V)$, were performed in a wide temperature range by Greywall.[16]

In view of the fundamental importance of liquid ^{3}He for our understanding of strongly correlated Fermi systems it would be desirable

(i) to have complete knowledge of all equilibrium thermodynamic quantities in the full (T,P) *and* (T,V) plane, and

(ii) to be sure that these values indeed fulfill the usual thermodynamic relations, i.e., are *thermodynamically consistent*.

In this paper we wish to point out that it is possible to *calculate* the full set of equilibrium thermodynamic quantities characterizing normal-liquid ^{3}He from the specific heat $C_V(T,V)$ measured by Greywall,[16] complemented by existing data for the molar volume $V(T_0,P)$ at a fixed temperature $T_0=0.1$ K as parametrized by Greywall.[16,17] Namely, these quantities are shown to contain the complete thermodynamic information about the system. This enables us to calculate all equilibrium thermodynamic quantities of liquid ^{3}He at zero magnetic field. The advantage of this approach is that the temperature and pressure (or volume) dependences of these quantities are then guaranteed to be thermodynamically consistent. These results are collected into figures and tables and provide the first complete set of thermodynamically consistent values of the equilibrium quantities of normal-liquid ^{3}He.

In this paper we deal only with the normal-liquid phase of ^{3}He. Nevertheless, since the measurements by Greywall[16] were performed down to temperatures as low as 7 mK, we will present also limiting values for thermodynamic quantities in the limit $T\to 0$, even though ^{3}He would be superfluid then. We note that Greywall later also published measurements of the specific heat and the melting curve of ^{3}He based on a revised temperature scale.[18,19] In order to maintain the thermodynamic consistency and since the new temperature scale leads to corrections[18] in $C_V(T,V)$ of only 0.5% above 0.07 K and 1% below 0.07 K, the calculations in this paper are based solely on the data of Ref. 16.

The paper is organized as follows. In Sec. II it is shown how to obtain the complete thermodynamic information from the known experimental data. In Sec. III the calculation of thermodynamic quantities is explained in some detail. In Sec. IV the molar volume $V(T,P)$, entropy $S(T,P)$, specific heat at constant pressure $C_P(T,P)$, compressibility $\kappa(T,P)$, and expansion coefficient $\alpha(T,P)$ are discussed, and are plotted and listed in tables.

II. COMPLETE THERMODYNAMIC INFORMATION

A thermodynamic potential as a function of its natural variables contains the complete thermodynamic information about the system in equilibrium. Here we show how to obtain the free energy $F(T,V)$ as a function of its natural variables T and V, when the specific heat $C_V(T,V)$ and the molar volume $V(T_0,P)$ at a fixed temperature T_0 are known. Since $dF=-S\,dT-P\,dV$, and hence

$$F(T,V)=-\int_{V_0}^{V} dV'\,P(T_0,V')-\int_{T_0}^{T} dT'\,S(T',V)+\text{const}, \tag{1}$$

one needs the entropy $S(T,V)$ and the pressure $P(T_0,V)$ to calculate $F(T,V)$. The entropy is obtained from $C_V(T,V)$ by integration:

$$S(T,V)=\int_0^T \frac{dT'}{T'} C_V(T',V), \tag{2}$$

and $P(T_0,V)$ can, in principle, be calculated from the molar volume $V(T_0,P)$ by inversion. In the following we will not calculate the free energy explicitly according to Eq. (1). Instead, we make use of the Maxwell relation

$$\left(\frac{\partial P}{\partial T}\right)_V = \left(\frac{\partial S}{\partial V}\right)_T \tag{3}$$

to obtain the pressure

$$P(T,V)=P(T_0,V)+\int_{T_0}^T dT' \left(\frac{\partial S(T',V)}{\partial V}\right)_{T'}, \tag{4}$$

and hence by inversion the molar volume $V(T,P)$. Equation (4) contains a central observation of this paper: $P(T_0,V)$ or $V(T_0,P)$ at a single temperature can be extended to all temperatures if $C_V(T,V)$ is known.

From these equations thermodynamic quantities such as the entropy $S(T,P)$ as well as derivatives of $V(T,P)$, such as the compressibility κ and the expansion coefficient α, can be calculated as functions of pressure (instead of volume) and temperature.

III. CALCULATION OF THERMODYNAMIC QUANTITIES

Based on his measurements, Greywall[16] provided interpolation formulas $c_1(T,V)$, $c_2(T,V)$, and $v_0(P)$, representing the specific heat at constant volume $C_V(T,V)$:

$$\frac{1}{R} C_V(T,V)=\begin{cases} c_1(T,V) & \text{for } T<T_0 \\ c_2(T,V) & \text{for } T\geqslant T_0, \end{cases} \tag{5}$$

as well as the molar volume $V(T_0,P)$ at temperature $T_0=0.1$ K:

$$V(T_0,P)=v_0(P). \tag{6}$$

Greywall fitted the interpolation formulas in the temperature range $0.007\leqslant T\leqslant 2.5$ K for molar volumes $26.169\leqslant V\leqslant 36.820$ cm^3. His interpolation formulas are given by

$$c_1(T,V)=\sum_{i=1}^{5}\sum_{j=0}^{3} a_{ij}\frac{T^i}{V^j}, \tag{7}$$

$$c_2(T,V)=\sum_{i=0}^{3}\sum_{j=0}^{2} [b_{ij}+c_{ij}\, e^{-d(V)/T}]\,\frac{V^j}{T^i}, \tag{8}$$

$$v_0(P)=\sum_{i=0}^{5} a_i P^i, \tag{9}$$

with $d(V)=\Sigma_{j=0}^{2} d_j V^j$. Here and in the following T, V, and P are in units of K, cm^3, and bar, respectively. Below we will also need the inverse of Eq. (6), i.e., $p_0(V)=P(T_0,V)$. We use the function

$$p_0(V)=\sum_{i=1}^{7} b_i (V-a_0)^i, \tag{10}$$

which we fitted to the inverse of $v_0(P)$ by a least-square fit (rms deviation 0.2 bar).[20] The parameters b_i, as well as Greywall's parameters appearing in Eqs. (7)–(9), are listed in Table I.

Using Eqs. (2) and (4) together with Eq. (5) we obtain the entropy $S(T,V)$ and pressure $P(T,V)$ as

$$\frac{1}{R} S(T,V)=\begin{cases} s_1(T,V) & \text{for } T<T_0 \\ s_2(T,V)+s_1(T_0,V)-s_2(T_0,V) & \text{for } T\geqslant T_0, \end{cases} \tag{11}$$

TABLE I. Coefficients entering the interpolation formulas (Ref. 16) for the specific heat [Eqs. (7) and (8)], the molar volume [Eq. (9)], and the least-square fit for the pressure [Eq. (10)].

	$j=0$	$j=1$	$j=2$	$j=3$
a_{1j}	-2.9190414	5.2893401×10^{2}	-1.8869641×10^{4}	2.6031315×10^{5}
a_{3j}	-2.4752597×10^{3}	1.8377260×10^{5}	-3.4946553×10^{6}	0
a_{4j}	3.8887481×10^{4}	-2.8649769×10^{6}	5.2526785×10^{7}	0
a_{5j}	-1.7505655×10^{5}	1.2809001×10^{7}	-2.3037701×10^{8}	0
b_{0j}	-6.5521193×10^{-2}	1.3502371×10^{-2}	0	0
b_{1j}	4.1359033×10^{-2}	3.8233755×10^{-4}	-5.3468396×10^{-5}	0
b_{2j}	5.7976786×10^{-3}	-6.5611532×10^{-4}	1.2689707×10^{-5}	0
b_{3j}	-3.8374623×10^{-4}	3.2072581×10^{-5}	-5.3038906×10^{-7}	0
c_{1j}	-2.5482958×10^{1}	1.6416936	-1.5110378×10^{-2}	0
c_{2j}	3.7882751×10^{1}	-2.8769188	3.5751181×10^{-2}	0
c_{3j}	2.4412956×10^{1}	-2.4244083	6.7775905×10^{-2}	0
d_j	7.1613436	6.0525139×10^{-1}	-7.1295855×10^{-3}	0
a_j	3.6820×10^{1}	-1.2094	9.4231×10^{-2}	-4.9875×10^{-3}
a_{j+4}	1.3746×10^{-4}	-1.4756×10^{-6}	0	0
b_j	0	-8.3094892×10^{-1}	6.1583050×10^{-2}	-4.5946040×10^{-3}
b_{j+4}	1.7370990×10^{-4}	-3.8137958×10^{-5}	2.3397112×10^{-6}	1.7579799×10^{-7}

$$P(T,V)=\begin{cases} p_0(V)+q\,[p_1(T,V)-p_1(T_0,V)] & \text{for } T<T_0 \\ p_0(V)+q\,[p_2(T,V)-p_2(T_0,V)] & \\ \quad +(T-T_0)\,q\,\dfrac{\partial}{\partial V}[s_1(T_0,V)-s_2(T_0,V)] & \text{for } T\geqslant T_0, \end{cases} \tag{12}$$

where the auxiliary functions $s_i(T,V)$ and $p_i(T,V)$ are defined for $i=1,2$ via $\partial s_i/\partial T=c_i/T$, $\partial s_i/\partial V=\partial p_i/\partial T$, with $s_1(0,V)=0$, and q is a conversion factor, $q=83.1451$. After analytically performing the necessary integrations we obtain the following expressions:

$$s_1(T,V)=\sum_{i=1}^{5}\sum_{j=0}^{3}\frac{a_{ij}}{i}\frac{T^i}{V^j}, \tag{13}$$

$$p_1(T,V)=-\sum_{i=1}^{5}\sum_{j=0}^{3}\frac{j\,a_{ij}}{i(i+1)}\frac{T^{i+1}}{V^{j+1}}, \tag{14}$$

$$s_2(T,V)=\sum_{j=0}^{2}\left[b_{0j}\ln T-\sum_{i=1}^{3}\frac{b_{ij}}{i}\frac{1}{T^i}+\sum_{i=0}^{2}\sum_{k=i+1}^{3}\frac{(k-1)!\,c_{kj}}{i!\,d(V)^{k-i}\,T^i}e^{-d(V)/T}\right]V^j, \tag{15}$$

$$\begin{aligned} p_2(T,V)=\sum_{j=1}^{2}\Bigg\{&(b_{0j}T-b_{1j})\ln T-b_{0j}T \\ &+\sum_{i=2}^{3}\frac{b_{ij}}{i(i-1)}\frac{1}{T^{i-1}}+\sum_{k=1}^{3}\frac{(k-1)!\,c_{kj}}{d(V)^{k-1}} \\ &\times\left[\left(\frac{T}{d(V)}+\frac{1}{2}\delta_{k3}\right)e^{-d(V)/T}+\delta_{k1}\,\mathrm{Ei}\left(-\frac{d(V)}{T}\right)\right]\Bigg\} \\ &\times j\,V^{j-1}+\sum_{j=0}^{2}\sum_{k=1}^{3}\frac{(k-1)!\,c_{kj}}{d(V)^k}\left[1-k\right. \\ &\left.\times\left(1+\frac{T}{d(V)}\right)-\delta_{k3}\frac{d(V)}{2T}\right]e^{-d(V)/T}d'(V)V^j. \end{aligned} \tag{16}$$

The only nonelementary function that appears in these expressions is the exponential integral $\mathrm{Ei}(x)$, defined by

$$\mathrm{Ei}(-x)=-\int_x^\infty\frac{dt}{t}e^{-t},\quad x>0. \tag{17}$$

This function can be calculated numerically without difficulty.[21]

Other thermodynamic quantities can be calculated from Eqs. (5), (11), and (12). The specific heat at constant pressure C_P is given by

$$C_P(T,P)=T\left(\frac{\partial S}{\partial T}\right)_P=T\left(\frac{\partial S}{\partial T}\right)_V-T\frac{\left(\dfrac{\partial P}{\partial T}\right)_V^2}{\left(\dfrac{\partial P}{\partial V}\right)_T}, \tag{18}$$

and the isothermal compressibility and isobaric expansion coefficient are calculated from Eq. (12) as

$$\kappa(T,P)=-\frac{1}{V}\left(\frac{\partial V}{\partial P}\right)_T=-\frac{1}{V}\left(\frac{\partial P}{\partial V}\right)_T^{-1}, \tag{19}$$

$$\alpha(T,P)=\frac{1}{V}\left(\frac{\partial V}{\partial T}\right)_P=\kappa\left(\frac{\partial P}{\partial T}\right)_V. \tag{20}$$

After obtaining $V(T,P)$ from Eq. (12) by inversion, these quantities can be calculated as a function of T and P. It is also possible to calculate higher derivatives in terms of known functions by repeatedly applying standard thermodynamic relations, e.g.,

$$\left(\frac{\partial\kappa}{\partial P}\right)_T=\kappa^2-V^2\kappa^3\left(\frac{\partial^2P}{\partial V^2}\right)_T, \tag{21}$$

$$\left(\frac{\partial\kappa}{\partial T}\right)_P=-\kappa\,\alpha+V\kappa^2\alpha\left(\frac{\partial^2P}{\partial V^2}\right)_T+V\kappa^2\left(\frac{\partial^2S}{\partial V^2}\right)_T, \tag{22}$$

$$\left(\frac{\partial\alpha}{\partial P}\right)_T=-\left(\frac{\partial\kappa}{\partial T}\right)_P, \tag{23}$$

$$\begin{aligned} \left(\frac{\partial\alpha}{\partial T}\right)_P=&-\alpha^2+V^2\kappa\,\alpha^2\left(\frac{\partial^2P}{\partial V^2}\right)_T \\ &+2\,V\kappa\,\alpha\left(\frac{\partial^2S}{\partial V^2}\right)_T+\kappa\left(\frac{\partial^2P}{\partial T^2}\right)_V. \end{aligned} \tag{24}$$

Of these higher derivatives we will only evaluate the pressure dependence of $(\partial\alpha/\partial T)_P$ in the limit $T\to0$.

IV. RESULTS AND DISCUSSION

In this section we will present both figures and tables of thermodynamic quantities calculated by the procedure described above. The allowed temperature range for these interpolation formulas is $0\leqslant T\leqslant2.5$ K, where $T=0$ denotes the extrapolation of the Fermi-liquid data at $T=7$ mK to zero temperature, disregarding the occurrence of superfluid phases. The allowed range of molar volumes is $26.16\leqslant V\leqslant36.85$ cm^3. Note that for low molar volumes the pressure is always below the minimum of the melting pressure[22,16] at

TABLE II. Thermodynamic functions for normal-liquid ^{3}He at pressure $P=0$ bar. See also the discussion of the accuracy of $(\partial V/\partial T)_P$ at low pressures in Sec. IV C and Ref. 23.

T [K]	S/R	C_P/RT [K^{-1}]	V [cm^3]	$-(\partial V/\partial P)_T$ [$cm^3\,bar^{-1}$]	κ [10^{-2} bar^{-1}]	α [10^{-3} K^{-1}]
0	0	2.7411	36.8461	1.2062	3.27375	0
0.005	0.0137	2.7395	36.8460	1.2062	3.27374	−0.80
0.010	0.0274	2.7348	36.8458	1.2062	3.27372	−1.60
0.020	0.0547	2.7156	36.8449	1.2062	3.27364	−3.17
0.030	0.0817	2.6835	36.8435	1.2061	3.27348	−4.70
0.040	0.1083	2.6390	36.8415	1.2059	3.27322	−6.15
0.060	0.1599	2.5193	36.8360	1.2054	3.27228	−8.77
0.080	0.2089	2.3753	36.8287	1.2046	3.27070	−10.91
0.100	0.2550	2.2376	36.8200	1.2034	3.26845	−12.59
0.150	0.3595	1.9337	36.7959	1.2005	3.26267	−13.35
0.200	0.4485	1.6378	36.7718	1.1979	3.25765	−12.62
0.250	0.5242	1.4004	36.7499	1.1956	3.25341	−11.08
0.300	0.5895	1.2160	36.7313	1.1938	3.25020	−9.16
0.350	0.6465	1.0716	36.7164	1.1926	3.24815	−7.09
0.400	0.6971	0.9570	36.7053	1.1920	3.24736	−4.99
0.450	0.7426	0.8652	36.6981	1.1919	3.24788	−2.91
0.500	0.7839	0.7913	36.6946	1.1925	3.24973	−0.90
0.600	0.8573	0.6834	36.6984	1.1955	3.25751	2.94
0.700	0.9219	0.6129	36.7160	1.2010	3.27100	6.63
0.800	0.9807	0.5661	36.7471	1.2092	3.29069	10.35
0.900	1.0356	0.5343	36.7923	1.2205	3.31734	14.27

TABLE III. Thermodynamic functions for normal-liquid ^{3}He at pressure $P=5$ bar.

T [K]	S/R	C_P/RT [K^{-1}]	V [cm^3]	$-(\partial V/\partial P)_T$ [$cm^3\,bar^{-1}$]	κ [10^{-2} bar^{-1}]	α [10^{-3} K^{-1}]
0	0	3.0586	32.6559	0.5863	1.79539	0
0.005	0.0153	3.0555	32.6558	0.5863	1.79539	−0.74
0.010	0.0305	3.0466	32.6556	0.5863	1.79539	−1.47
0.020	0.0609	3.0124	32.6549	0.5863	1.79536	−2.86
0.030	0.0907	2.9589	32.6538	0.5862	1.79531	−4.14
0.040	0.1200	2.8891	32.6522	0.5862	1.79523	−5.29
0.060	0.1761	2.7147	32.6481	0.5860	1.79496	−7.14
0.080	0.2284	2.5199	32.6430	0.5858	1.79455	−8.46
0.100	0.2770	2.3232	32.6372	0.5855	1.79401	−9.35
0.150	0.3835	1.9367	32.6208	0.5847	1.79246	−10.41
0.200	0.4715	1.5987	32.6040	0.5839	1.79098	−10.07
0.250	0.5448	1.3426	32.5883	0.5833	1.78982	−9.15
0.300	0.6069	1.1507	32.5743	0.5828	1.78913	−7.99
0.350	0.6606	1.0043	32.5623	0.5825	1.78897	−6.75
0.400	0.7078	0.8905	32.5523	0.5825	1.78937	−5.51
0.450	0.7500	0.8009	32.5443	0.5827	1.79035	−4.32
0.500	0.7882	0.7298	32.5382	0.5831	1.79189	−3.18
0.600	0.8557	0.6268	32.5313	0.5845	1.79665	−1.09
0.700	0.9147	0.5582	32.5310	0.5867	1.80350	0.85
0.800	0.9680	0.5102	32.5369	0.5897	1.81231	2.78
0.900	1.0172	0.4749	32.5491	0.5934	1.82304	4.79
1.000	1.0633	0.4481	32.5681	0.5979	1.83573	6.92
1.200	1.1489	0.4112	32.6282	0.6094	1.86756	11.58
1.400	1.2287	0.3892	32.7203	0.6248	1.90941	16.68
1.600	1.3052	0.3767	32.8474	0.6449	1.96331	22.13
1.800	1.3798	0.3705	33.0121	0.6707	2.03183	27.95
2.000	1.4537	0.3687	33.2178	0.7037	2.11835	34.28
2.500	1.6398	0.3794	33.9491	0.8327	2.45273	54.08

TABLE IV. Thermodynamic functions for normal-liquid ^{3}He at pressure $P=10$ bar.

T [K]	S/R	C_P/RT [K^{-1}]	V [cm^3]	$-(\partial V/\partial P)_T$ [$cm^3\,bar^{-1}$]	κ [10^{-2} bar^{-1}]	α [10^{-3} K^{-1}]
0	0	3.3313	30.3745	0.3587	1.18080	0
0.005	0.0166	3.3261	30.3744	0.3587	1.18080	−0.71
0.010	0.0332	3.3115	30.3743	0.3587	1.18079	−1.40
0.020	0.0661	3.2580	30.3737	0.3586	1.18078	−2.72
0.030	0.0983	3.1784	30.3726	0.3586	1.18076	−3.92
0.040	0.1296	3.0799	30.3713	0.3586	1.18072	−4.96
0.060	0.1890	2.8510	30.3678	0.3585	1.18062	−6.60
0.080	0.2436	2.6136	30.3634	0.3584	1.18049	−7.74
0.100	0.2937	2.4003	30.3584	0.3583	1.18033	−8.50
0.150	0.4021	1.9436	30.3446	0.3580	1.17983	−9.42
0.200	0.4896	1.5765	30.3304	0.3577	1.17932	−9.23
0.250	0.5614	1.3089	30.3168	0.3574	1.17897	−8.60
0.300	0.6217	1.1127	30.3044	0.3572	1.17884	−7.81
0.350	0.6735	0.9656	30.2932	0.3572	1.17899	−6.96
0.400	0.7188	0.8529	30.2833	0.3572	1.17942	−6.13
0.450	0.7592	0.7653	30.2746	0.3573	1.18013	−5.35
0.500	0.7957	0.6964	30.2671	0.3575	1.18112	−4.61
0.600	0.8600	0.5967	30.2552	0.3582	1.18388	−3.26
0.700	0.9161	0.5290	30.2472	0.3592	1.18756	−1.99
0.800	0.9664	0.4799	30.2432	0.3605	1.19204	−0.68
0.900	1.0124	0.4426	30.2432	0.3621	1.19724	0.72
1.000	1.0552	0.4136	30.2477	0.3639	1.20316	2.23
1.200	1.1335	0.3732	30.2709	0.3685	1.21735	5.50
1.400	1.2055	0.3489	30.3146	0.3744	1.23512	8.93
1.600	1.2738	0.3347	30.3793	0.3819	1.25707	12.42
1.800	1.3398	0.3263	30.4656	0.3911	1.28378	15.94
2.000	1.4045	0.3213	30.5737	0.4023	1.31592	19.51
2.500	1.5636	0.3162	30.9456	0.4412	1.42576	29.06

TABLE V. Thermodynamic functions for normal-liquid ^{3}He at pressure $P=15$ bar.

T [K]	S/R	C_P/RT [K^{-1}]	V [cm^3]	$-(\partial V/\partial P)_T$ [$cm^3\,bar^{-1}$]	κ [10^{-2} bar^{-1}]	α [10^{-3} K^{-1}]
0	0	3.5803	28.8722	0.2540	0.87982	0
0.005	0.0179	3.5731	28.8721	0.2540	0.87982	−0.69
0.010	0.0357	3.5528	28.8720	0.2540	0.87982	−1.38
0.020	0.0709	3.4799	28.8714	0.2540	0.87982	−2.67
0.030	0.1052	3.3747	28.8704	0.2540	0.87982	−3.84
0.040	0.1383	3.2487	28.8692	0.2540	0.87981	−4.86
0.060	0.2005	2.9696	28.8659	0.2540	0.87980	−6.45
0.080	0.2572	2.6959	28.8618	0.2539	0.87979	−7.56
0.100	0.3086	2.4629	28.8572	0.2539	0.87979	−8.33
0.150	0.4185	1.9504	28.8444	0.2538	0.87975	−9.14
0.200	0.5058	1.5617	28.8313	0.2536	0.87969	−9.02
0.250	0.5766	1.2859	28.8186	0.2535	0.87972	−8.54
0.300	0.6356	1.0870	28.8067	0.2535	0.87988	−7.94
0.350	0.6861	0.9397	28.7958	0.2535	0.88019	−7.30
0.400	0.7302	0.8282	28.7857	0.2535	0.88066	−6.69
0.450	0.7694	0.7423	28.7765	0.2536	0.88129	−6.11
0.500	0.8047	0.6749	28.7681	0.2538	0.88208	−5.58
0.600	0.8670	0.5771	28.7535	0.2542	0.88407	−4.60
0.700	0.9211	0.5091	28.7416	0.2548	0.88652	−3.62
0.800	0.9694	0.4584	28.7327	0.2555	0.88934	−2.56
0.900	1.0132	0.4192	28.7270	0.2564	0.89246	−1.39
1.000	1.0535	0.3885	28.7248	0.2573	0.89588	−0.13
1.200	1.1266	0.3463	28.7318	0.2597	0.90374	2.58
1.400	1.1932	0.3216	28.7546	0.2626	0.91318	5.36
1.600	1.2559	0.3073	28.7933	0.2662	0.92445	8.10
1.800	1.3165	0.2989	28.8478	0.2705	0.93777	10.78
2.000	1.3757	0.2936	28.9177	0.2757	0.95333	13.42
2.500	1.5203	0.2856	29.1603	0.2927	1.00366	20.02

TABLE VI. Thermodynamic functions for normal-liquid ^{3}He at pressure $P=20$ bar.

T [K]	S/R	C_P/RT [K^{-1}]	V [cm^3]	$-(\partial V/\partial P)_T$ [$cm^3\,bar^{-1}$]	κ [10^{-2} bar^{-1}]	α [10^{-3} K^{-1}]
0	0	3.8176	27.7571	0.1971	0.70992	0
0.005	0.0191	3.8083	27.7571	0.1971	0.70992	−0.70
0.010	0.0381	3.7824	27.7569	0.1971	0.70992	−1.39
0.020	0.0755	3.6907	27.7563	0.1971	0.70993	−2.69
0.030	0.1117	3.5610	27.7554	0.1970	0.70994	−3.86
0.040	0.1466	3.4086	27.7542	0.1970	0.70995	−4.89
0.060	0.2115	3.0828	27.7510	0.1970	0.70999	−6.50
0.080	0.2701	2.7768	27.7471	0.1970	0.71005	−7.65
0.100	0.3228	2.5156	27.7426	0.1970	0.71013	−8.48
0.150	0.4341	1.9567	27.7302	0.1970	0.71033	−9.20
0.200	0.5211	1.5507	27.7174	0.1969	0.71051	−9.12
0.250	0.5912	1.2686	27.7051	0.1969	0.71075	−8.73
0.300	0.6493	1.0678	27.6933	0.1969	0.71107	−8.24
0.350	0.6989	0.9206	27.6822	0.1970	0.71149	−7.74
0.400	0.7420	0.8102	27.6719	0.1970	0.71201	−7.25
0.450	0.7803	0.7257	27.6622	0.1971	0.71264	−6.80
0.500	0.8149	0.6595	27.6530	0.1973	0.71337	−6.39
0.600	0.8757	0.5624	27.6365	0.1976	0.71508	−5.61
0.700	0.9283	0.4932	27.6221	0.1981	0.71704	−4.78
0.800	0.9748	0.4405	27.6102	0.1986	0.71917	−3.83
0.900	1.0168	0.3995	27.6011	0.1991	0.72144	−2.76
1.000	1.0550	0.3675	27.5950	0.1997	0.72384	−1.61
1.200	1.1238	0.3242	27.5929	0.2012	0.72912	0.85
1.400	1.1860	0.2996	27.6044	0.2029	0.73517	3.32
1.600	1.2444	0.2860	27.6294	0.2050	0.74214	5.72
1.800	1.3007	0.2781	27.6674	0.2075	0.75012	8.02
2.000	1.3558	0.2731	27.7180	0.2104	0.75920	10.24
2.500	1.4901	0.2647	27.8980	0.2196	0.78725	15.62

$P\approx 29.3$ bar and $T\approx 0.32$ K. For high molar volumes the volume range includes the point $V(T=0,P=0)\approx 36.85$ cm^3, this representing a slight extrapolation of Greywall's original formulas which extended only to $V=36.82$ cm^3. The resulting range of pressures is $0\leqslant P\lesssim 28$–29 bar, depending on temperature.

Below we present results for the molar volume, entropy, and specific heat as a function of pressure and temperature, as well as the first derivatives of the molar volume, the compressibility, and the thermal expansion coefficient.[23] Using Eqs. (21)–(24) of Sec. III it is also possible, in principle, to calculate higher derivatives, but because their reliability is difficult to judge we will calculate only the slope of the expansion coefficient as a function of pressure for $T\to 0$.

For pressures 0, 5, 10, 15, 20, 25, and 28 bar, Tables II–VIII show data vs T at temperatures $0\leqslant T\leqslant 2.5$ K. Table IX lists data vs P at $T=0$. We note that, for $P=0$, calculations are restricted to $T<1$ K since at higher temperatures the calculated molar volumes $V(T,P=0)$ become larger than 36.85 cm^3 and are thus outside the regime of the interpolation formulas. We also note that since the interpolation formulas are given by two different expressions for temperatures above and below $T=0.1$ K, there appear weak cusps or discontinuities in some of the curves at this temperature, which we purposely did not smooth out.

A. Molar volume $V(T,P)$

The temperature dependence of the molar volume $V(T,P)$ is plotted in Fig. 1 relative to its zero-temperature value. The pressure dependence of $V(T,P)$ is shown in Fig. 2 for $T=0,1,2$ K. The change in volume over the temperature range 0–2.5 K is small ($\lesssim 4\%$).

At low temperatures the volume is seen to *decrease* upon increase of temperature, implying a negative thermal expansion coefficient. This is found in many strongly correlated fermion systems and is due to the anomalous *increase* of entropy with pressure in these systems as will be discussed in the following two subsections.

In the limit $T\to 0$ we compared our results for $V(0,P)$ (see also Table IX) with the values determined by Wheatley.[5] We find very good agreement for all pressures, the relative difference between these values being less than 0.5%. At higher temperatures ($1\leqslant T\leqslant 2.4$ K) our evaluation of $V(T,P)$ can be compared to the corrected data of Sherman and Edeskuty,[10] which are tabulated in Wilks' book.[6] Again the agreement is very good for all pressures, with relative differences less than 0.6%. Comparison with the data of Abraham and Osborne[15] also shows very good agreement, with relative differences of at most 0.3%.

TABLE VII. Thermodynamic functions for normal-liquid ^{3}He at pressure $P=25$ bar.

T [K]	S/R	C_P/RT [K^{-1}]	V [cm^3]	$-(\partial V/\partial P)_T$ [$cm^3\,bar^{-1}$]	κ [10^{-2} bar^{-1}]	α [10^{-3} K^{-1}]
0	0	4.0499	26.8659	0.1620	0.60283	0
0.005	0.0202	4.0386	26.8659	0.1620	0.60283	−0.71
0.010	0.0404	4.0072	26.8657	0.1620	0.60284	−1.42
0.020	0.0799	3.8972	26.8652	0.1620	0.60285	−2.75
0.030	0.1182	3.7436	26.8643	0.1620	0.60287	−3.95
0.040	0.1547	3.5658	26.8630	0.1620	0.60289	−5.00
0.060	0.2223	3.1956	26.8599	0.1620	0.60296	−6.66
0.080	0.2828	2.8597	26.8560	0.1620	0.60306	−7.88
0.100	0.3370	2.5617	26.8515	0.1620	0.60320	−8.79
0.150	0.4493	1.9626	26.8391	0.1620	0.60354	−9.46
0.200	0.5363	1.5421	26.8264	0.1620	0.60387	−9.40
0.250	0.6058	1.2547	26.8140	0.1620	0.60425	−9.07
0.300	0.6632	1.0525	26.8021	0.1621	0.60468	−8.66
0.350	0.7119	0.9057	26.7908	0.1621	0.60518	−8.24
0.400	0.7544	0.7964	26.7800	0.1622	0.60576	−7.85
0.450	0.7920	0.7130	26.7698	0.1623	0.60641	−7.49
0.500	0.8260	0.6476	26.7600	0.1625	0.60713	−7.15
0.600	0.8856	0.5502	26.7417	0.1628	0.60875	−6.49
0.700	0.9369	0.4792	26.7254	0.1632	0.61052	−5.73
0.800	0.9819	0.4244	26.7112	0.1636	0.61236	−4.84
0.900	1.0221	0.3816	26.6996	0.1640	0.61426	−3.82
1.000	1.0586	0.3485	26.6909	0.1645	0.61622	−2.70
1.200	1.1235	0.3045	26.6827	0.1655	0.62033	−0.37
1.400	1.1817	0.2805	26.6869	0.1668	0.62484	1.95
1.600	1.2364	0.2676	26.7033	0.1682	0.62983	4.16
1.800	1.2891	0.2605	26.7312	0.1698	0.63535	6.27
2.000	1.3408	0.2560	26.7702	0.1717	0.64144	8.29
2.500	1.4667	0.2480	26.9138	0.1775	0.65936	13.08

B. Entropy $S(T,P)$ and specific heat $C_P(T,P)$

In Fig. 3 $S(T,P)/T$ is shown as a function of temperature for several values of pressure. In Fig. 4 $S(T,P)$ is plotted as a function of pressure, relative to its value at $P=0$ shown as an inset. Comparison of Fig. 4 with earlier, independent measurements[9,11] of the entropy shows good quantitative agreement.

The specific heat $C_P(T,P)$ is plotted as a function of temperature in Figs. 5 and 6, and as a function of pressure in Fig. 7. As expected, the difference between the values of the specific heat at constant pressure C_P and the previously published[16] data at constant volume C_V is very small for low temperatures. However, at the highest available temperature, $T=2.5$ K, this difference increases to about 10%.[24]

At very low temperatures ^{3}He is a Landau Fermi liquid[2] with an entropy and specific heat linear in T,

$$S(T,P)=C_P(T,P)=\gamma(P)RT, \quad T\to 0. \tag{25}$$

The coefficient γ can be expressed in terms of the effective mass m^* or the Landau parameter F_1^s as

$$\frac{\gamma}{\gamma_0}=\frac{m^*}{m}=1+\frac{1}{3}F_1^s, \tag{26}$$

where[5]

$$\gamma_0=\frac{\pi^2 k_B m}{\hbar^2}\left(\frac{V(0,P)}{3\pi^2 N}\right)^{2/3}=8.991\times 10^{-2}\ \mathrm{K}^{-1}\left(\frac{V(0,P)}{\mathrm{cm}^3}\right)^{2/3} \tag{27}$$

is the corresponding coefficient of a hypothetical free fermion gas with atomic mass of ^{3}He, $m=5.009\times 10^{-24}$ g, at the same density. The behavior of $\gamma(P)$ and its derivative with respect to P are shown in Fig. 8. The Fermi liquid parameter F_1^s is plotted in Fig. 9 and compared to the values obtained by Greywall[16] from $\gamma(V)$ using $V(0.1\ \mathrm{K},P)$ instead of $V(0,P)$ in Eq. (27). The agreement is excellent, because the difference between $V(0.1\ \mathrm{K},P)$ and $V(0,P)$ is small.

The coefficient $\gamma(P)$ is seen to increase with pressure (see Fig. 8), implying that, at low temperatures, both the entropy $S(T,P)$ and the specific heat $C_P(T,P)$ increase with pressure: $(\partial S/\partial P)_T>0$, $(\partial C_P/\partial P)_T>0$. This may be attributed to the excitation of low-energy (spin) degrees of freedom in the correlated system.[25] The Maxwell relation

$$\left(\frac{\partial S}{\partial P}\right)_T=-\left(\frac{\partial V}{\partial T}\right)_P \tag{28}$$

then implies that at low temperatures $(\partial V/\partial T)_P<0$. This explains the effect discussed above, namely that the volume shrinks upon increase of T.

TABLE VIII. Thermodynamic functions for normal-liquid ^{3}He at pressure $P=28$ bar.

T [K]	S/R	C_P/RT [K^{-1}]	V [cm^3]	$-(\partial V/\partial P)_T$ [$cm^3\,bar^{-1}$]	κ [10^{-2} bar^{-1}]	α [10^{-3} K^{-1}]
0	0	4.1886	26.4036	0.1468	0.55603	0
0.005	0.0209	4.1762	26.4036	0.1468	0.55603	−0.73
0.010	0.0417	4.1415	26.4034	0.1468	0.55603	−1.44
0.020	0.0826	4.0207	26.4029	0.1468	0.55605	−2.80
0.030	0.1220	3.8529	26.4020	0.1468	0.55607	−4.03
0.040	0.1596	3.6603	26.4007	0.1468	0.55610	−5.10
0.060	0.2288	3.2643	26.3976	0.1468	0.55619	−6.81
0.080	0.2904	2.9113	26.3936	0.1468	0.55631	−8.07
0.100	0.3455	2.5870	26.3891	0.1468	0.55646	−9.03
0.150	0.4585	1.9660	26.3766	0.1469	0.55687	−9.68
0.200	0.5454	1.5377	26.3639	0.1469	0.55727	−9.63
0.250	0.6146	1.2476	26.3514	0.1470	0.55771	−9.33
0.300	0.6716	1.0446	26.3393	0.1470	0.55820	−8.96
0.350	0.7200	0.8981	26.3278	0.1471	0.55874	−8.58
0.400	0.7620	0.7895	26.3167	0.1472	0.55935	−8.22
0.450	0.7994	0.7068	26.3061	0.1473	0.56003	−7.91
0.500	0.8330	0.6416	26.2959	0.1475	0.56077	−7.61
0.600	0.8920	0.5437	26.2767	0.1478	0.56238	−7.00
0.700	0.9426	0.4714	26.2593	0.1481	0.56410	−6.27
0.800	0.9868	0.4153	26.2439	0.1485	0.56587	−5.39
0.900	1.0261	0.3714	26.2311	0.1489	0.56767	−4.37
1.000	1.0614	0.3377	26.2211	0.1493	0.56949	−3.27
1.200	1.1241	0.2934	26.2099	0.1502	0.57325	−0.98
1.400	1.1802	0.2698	26.2107	0.1513	0.57726	1.28
1.600	1.2328	0.2575	26.2231	0.1525	0.58160	3.43
1.800	1.2835	0.2508	26.2466	0.1539	0.58630	5.47
2.000	1.3333	0.2466	26.2804	0.1554	0.59136	7.42
2.500	1.4546	0.2391	26.4088	0.1600	0.60579	12.01

As noted before,[8,16] the specific-heat curves for different pressures P (or molar volumes V) cross sharply at $T_+ = 0.16$ K, a feature which is also observed in other strongly correlated systems.[25] In the case of ^{3}He the crossing of curves is due to the above-mentioned anomalous pressure dependence of the specific heat at low temperatures, where $(\partial C_P/\partial P)_T > 0$, and the free-fermion behavior $(\partial C_P/\partial P)_T < 0$ at higher temperatures (see Fig. 7), implying that at some intermediate temperature $T_+(P)$ the slope of C_P vs P vanishes, i.e., $(\partial C_P/\partial P)_{T_+} = 0$. Consequently, the curves C_P vs T cross at $T_+(P)$ (see Fig. 5). Furthermore, the curvature of C_P with respect to P

$$\left(\frac{\partial^2 C_P}{\partial P^2}\right)_T = -T\left(\frac{\partial^2}{\partial T^2}\right)_P \left(\frac{\partial V}{\partial P}\right)_T \tag{29}$$

is also small at T_+, since $(\partial V/\partial P)_T = -V\kappa$ itself is small and depends only weakly on temperature near T_+ (see below). Therefore at T_+ the curves C_P vs P are almost straight lines, implying an essentially *pressure independent* $T_+(P)$. The range of temperatures over which the crossing occurs is thus very narrow. In fact, the crossing region has a width $\Delta C_P/C_P \approx 0.5\%$ over the entire pressure range,[25] which cannot be resolved on the scale of Fig. 5, making it appear to be pointlike.

C. Derivatives of the molar volume

The results for the derivatives of V with respect to P and T are shown in Figs. 10 and 11. These quantities determine the compressibility and the thermal expansion coefficient.

Compressibility $\kappa(T,P)$

We now determine the isothermal compressibility $\kappa(T,P)$ [Eq. (19)] in a wide range of temperatures and pressures. The pressure dependence of κ is plotted for $T=0$, 1.5, 2.5 K in Fig. 12, while Figs. 13 and 14 show the temperature dependence of κ relative to its value at $T=0$. The variation of $\kappa(T,P)$ with temperature for a given pressure is rather small, except for high temperatures, where the deviation from $\kappa(0,P)$ can become quite large (see Fig. 12).

The zero-temperature value of the compressibility is connected to the Landau parameter F_0^s by[5]

$$\kappa(0,P) = \frac{9\pi^2 m^*}{\hbar^2(1+F_0^s)}\left(\frac{V(0,P)}{3\pi^2 N}\right)^{5/3} = 3.285\times 10^{-4}\ \text{bar}^{-1}\,\frac{m^*/m}{1+F_0^s}\left(\frac{V(0,P)}{\text{cm}^3}\right)^{5/3}. \tag{30}$$

TABLE IX. Pressure dependence of the molar volume V, linear coefficient of the specific heat $\gamma(P)$, its derivative $\gamma'(P)$, and compressibility κ, for $T\rightarrow 0$. See also the discussion of the accuracy of $(\partial V/\partial T)_P$ at low pressures in Sec. IV C and Ref. 23.

P [bar]	V [cm^3]	γ/R	$\frac{\partial\gamma}{\partial P}/R$ [10^{-2} bar^{-1}]	$\kappa(0,P)$ [10^{-2} bar^{-1}]
0	36.846	2.7411	7.1003	3.2737
1	35.739	2.8101	6.7192	2.8460
2	34.798	2.8758	6.4265	2.5032
3	33.986	2.9388	6.1884	2.2231
4	33.279	2.9996	5.9843	1.9905
5	32.656	3.0586	5.8046	1.7954
6	32.102	3.1158	5.6447	1.6306
7	31.605	3.1715	5.5025	1.4908
8	31.157	3.2259	5.3764	1.3715
9	30.749	3.2791	5.2650	1.2691
10	30.374	3.3313	5.1670	1.1808
11	30.030	3.3825	5.0810	1.1041
12	29.710	3.4329	5.0059	1.0371
13	29.412	3.4826	4.9404	0.9782
14	29.134	3.5317	4.8835	0.9261
15	28.872	3.5803	4.8343	0.8798
16	28.625	3.6285	4.7920	0.8385
17	28.392	3.6762	4.7558	0.8013
18	28.170	3.7236	4.7252	0.7678
19	27.959	3.7707	4.6995	0.7375
20	27.757	3.8176	4.6782	0.7099
21	27.564	3.8643	4.6610	0.6847
22	27.379	3.9108	4.6476	0.6617
23	27.202	3.9573	4.6375	0.6405
24	27.031	4.0036	4.6304	0.6209
25	26.866	4.0499	4.6263	0.6028
26	26.707	4.0961	4.6247	0.5861
27	26.553	4.1424	4.6256	0.5705
28	26.404	4.1886	4.6287	0.5560
29	26.259	4.2350	4.6340	0.5425

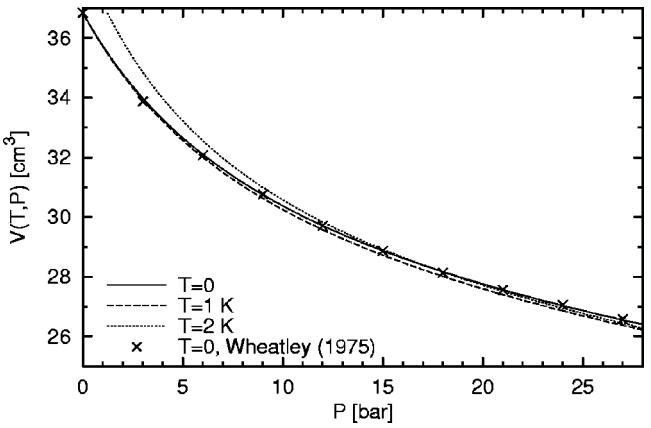

FIG. 2. Molar volume $V(T,P)$ vs P at temperatures $T=0$, 1, 2 K. The data of Wheatley (Ref. 5) at $T=0$ are also shown.

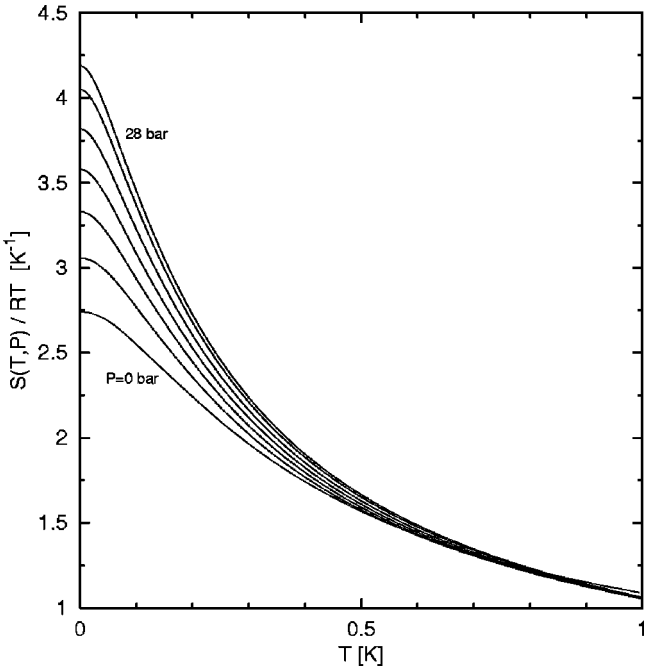

FIG. 3. Entropy $S(T,P)$ divided by temperature vs T at pressures $P=0$, 5, 10, 15, 20, 25, 28 bars.

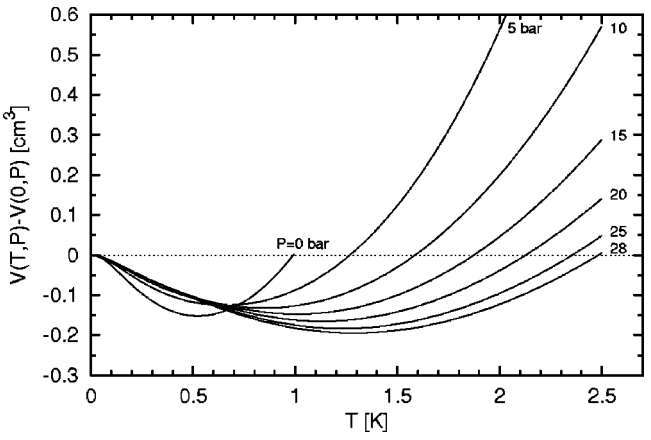

FIG. 1. Molar volume $V(T,P)$ vs T at several pressures P, plotted relative to its value at $T=0$ shown in Fig. 2.

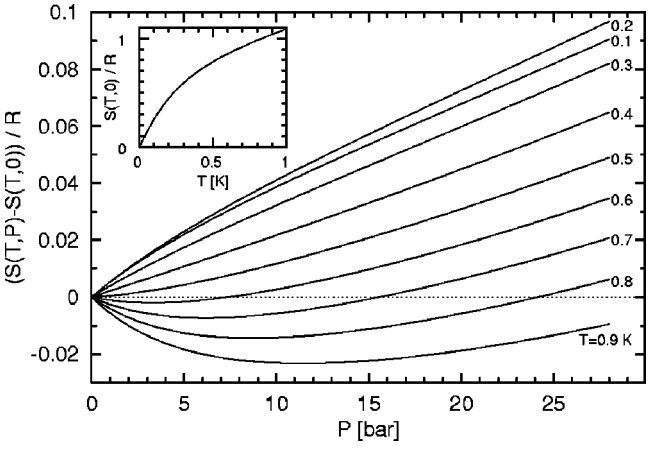

FIG. 4. Entropy $S(T,P)$ vs P at several temperatures T, plotted relative to its value at $P=0$ (inset).

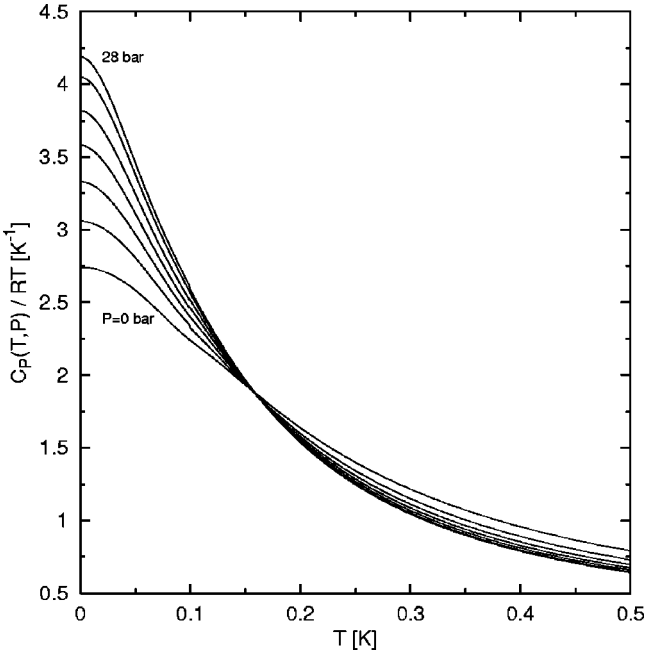

FIG. 5. Specific heat at constant pressure $C_P(T,P)$ divided by temperature vs T at pressures $P=0$, 5, 10, 15, 20, 25, 28 bar. The small kinks at the temperature $T_0=0.1$ K in this and other figures are artefacts caused by the different interpolation formulas (Ref. 16) for $C_V(T,V)$ used below and above T_0.

Using our evaluation of κ we can calculate F_0^s as a function of P, as shown in Fig. 15. Greywall's[16] data, obtained by adjusting Wheatley's values for F_0^s according to his new determination of m^*/m, are also shown. They are in good agreement with our evaluation.

We can also compare our evaluation of $\kappa(0,P)$ to that obtained from measurements of the sound velocity and molar volume as listed by Wheatley,[5] as well as to the data published by Abraham and Osborne[15] which they obtained by differentiating the molar volume. These data are included in Fig. 12. They agree well with our evaluation, with relative differences of at most 2%, except at very low pressures ($P \lesssim 2$ bar). At higher temperatures our evaluation of $\kappa(T,P)$ can again be compared to Abraham and Osborne's[15] data,

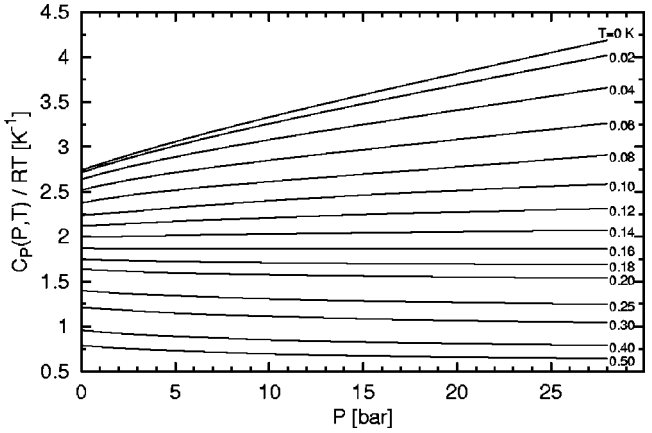

FIG. 7. Specific heat at constant pressure $C_P(T,P)$ divided by temperature vs P at several temperatures T. At $T_+=0.16$ K, $C_P(T,P)$ is essentially independent of pressure over the whole pressure range, leading to a sharp crossing point in the specific heat (see text).

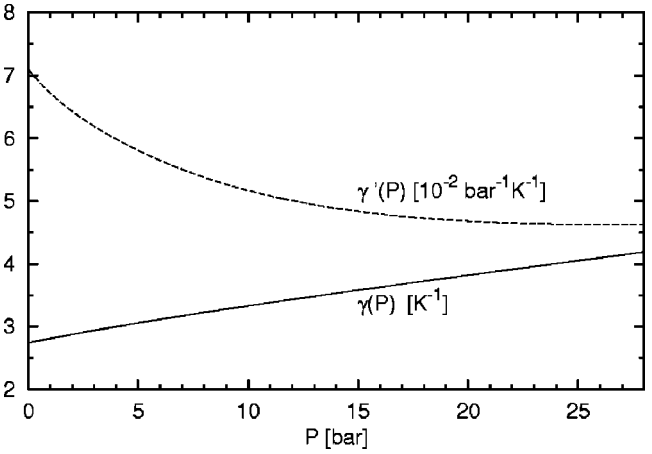

FIG. 8. Linear coefficient $\gamma(P)$ of the specific heat [Eq. (25)] vs P, and its derivative with respect to P, $\gamma'(P)$.

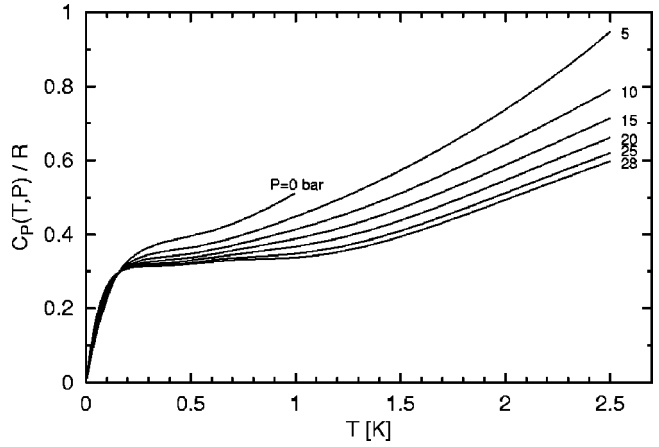

FIG. 6. High-temperature behavior of the specific heat at constant pressure $C_P(T,P)$.

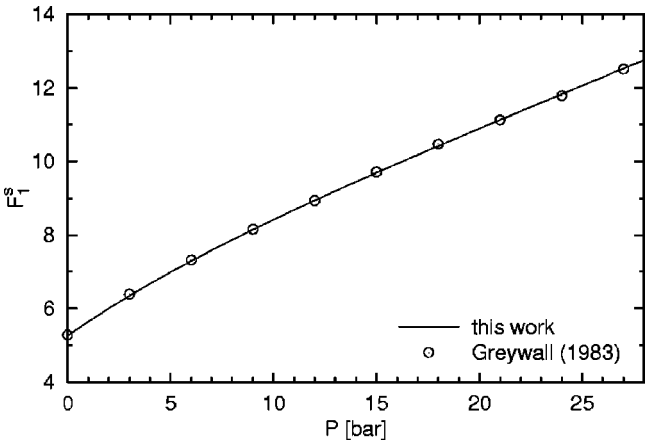

FIG. 9. Fermi-liquid parameter F_1^s vs P, compared to the data obtained by Greywall (Ref. 16).

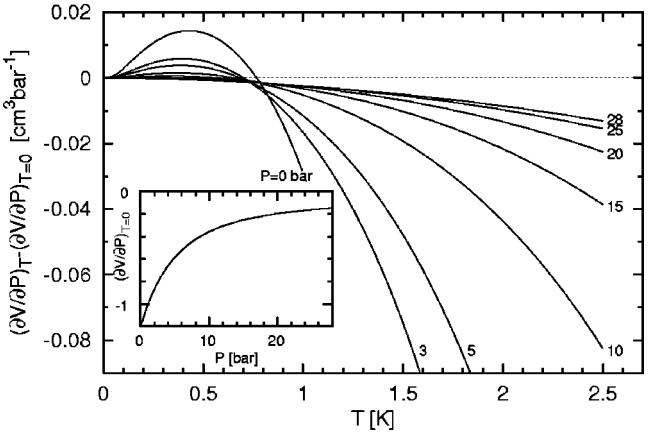

FIG. 10. Change of volume with pressure, $(\partial V/\partial P)_T$, vs T at several pressures, relative to its value at $T=0$ (inset).

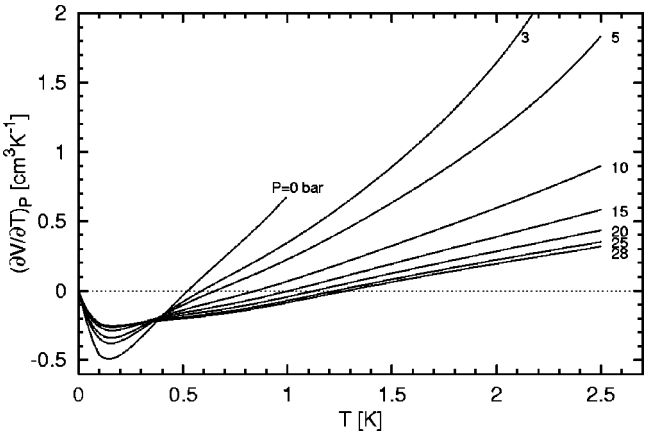

FIG. 11. Change of volume with temperature, $(\partial V/\partial T)_P$, vs T at several pressures P.

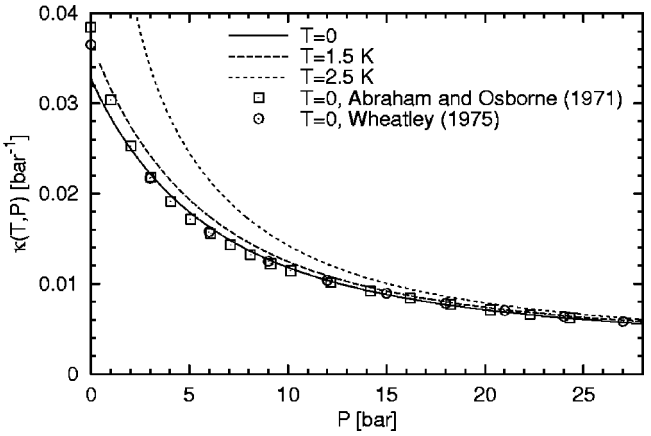

FIG. 12. Compressibility $\kappa(T,P)$ vs P at temperatures $T=0$, 1.5, 2.5 K, compared to the data at $T=0$ of Wheatley (Ref. 5) and Abraham and Osborne (Ref. 15).

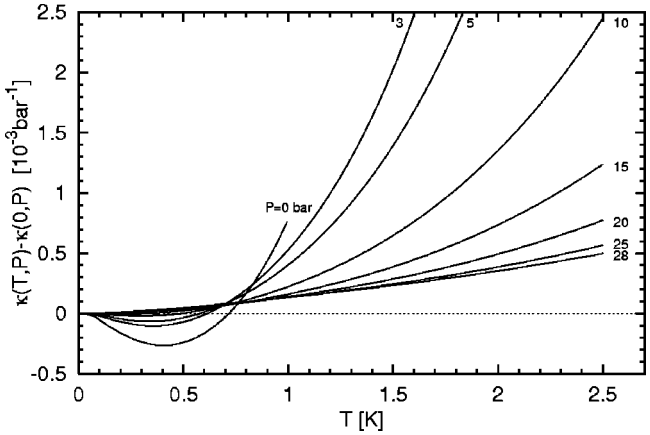

FIG. 13. Compressibility $\kappa(T,P)$ vs T at several pressures P, relative to its value at $T=0$ shown in Fig. 12.

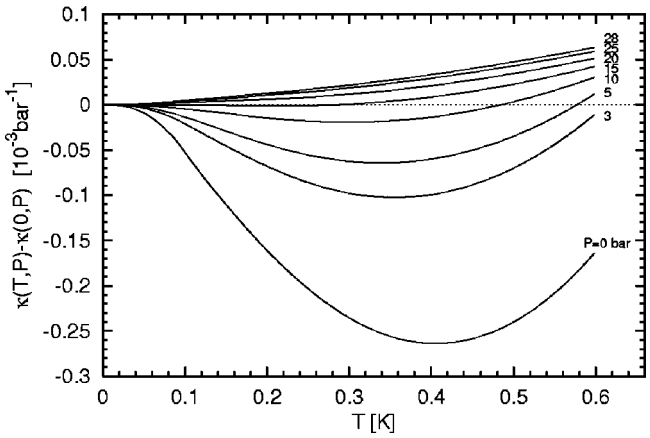

FIG. 14. Low-temperature behavior of the compressibility $\kappa(T,P)$ at several pressures P, relative to its value at $T=0$ (Fig. 12).

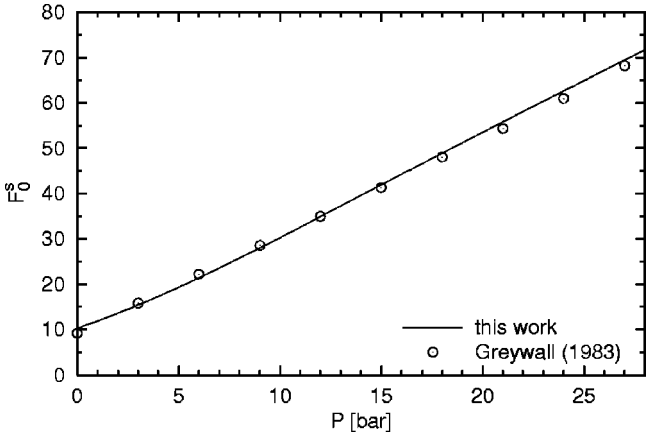

FIG. 15. Fermi-liquid parameter F_0^s as a function of pressure, compared to the data obtained by Greywall (Ref. 16) using Wheatley's (Ref. 5) values of $\kappa(0,P)$.

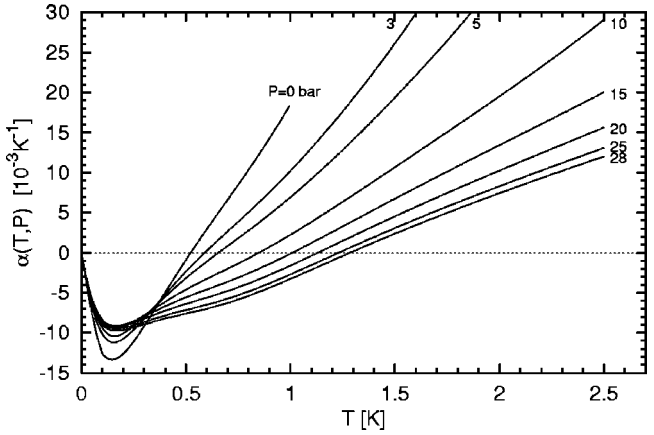

FIG. 16. Thermal expansion coefficient $\alpha(T,P)$ vs T at several pressures P.

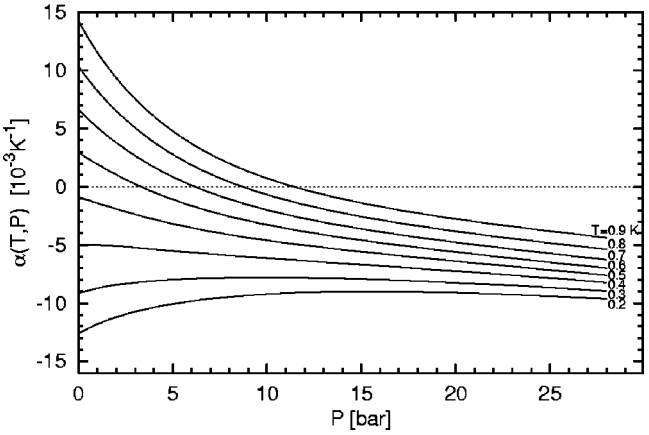

FIG. 18. Thermal expansion coefficient $\alpha(T,P)$ vs P at several temperatures T.

where we also find good agreement except for $P \lesssim 2$ bar. There is also good agreement with the data for $\kappa(T,P)$ published by Grilly.[14]

The difference at low pressures between our results for $\kappa(0,P)$ and other data, e.g., by Wheatley,[5] does not imply that any of Greywall's original data for C_V or his formula for $V(0.1\ \mathrm{K},P)$ are inaccurate. It merely indicates that our calculation of the *derivative* $(\partial V/\partial P)_T$ based on Greywall's interpolation formula for $V(T_0,P)$ may not be sufficiently accurate at low pressures.[23] Therefore the results for $\kappa(T,P)$ may indeed underestimate the pressure dependence of the molar volume at $P \lesssim 2$ bar.

Thermal expansion coefficient $\alpha(T,P)$

The temperature dependence of $\alpha(T,P)$ [Eq. (20)] is presented in Fig. 16, with Fig. 17 showing the low-temperature region in greater detail. The pressure dependence is plotted in Fig. 18.[26] Using Eq. (28) and the pressure dependence of $\gamma(P)$ the expansion coefficient is seen to be linear in T at very low temperatures,

$$\alpha(T,P) = -\frac{\gamma'(P)}{V(0,P)}T, \quad T \to 0, \tag{31}$$

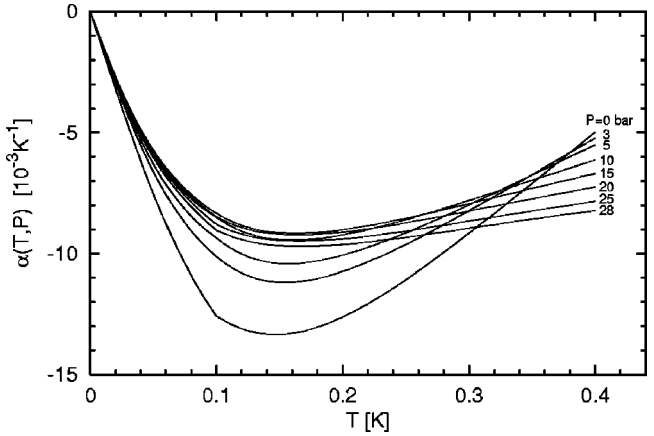

FIG. 17. Low-temperature behavior of the thermal expansion coefficient $\alpha(T,P)$ at several pressures P.

i.e., is *negative* and vanishes at $T=0$. The slope $(\partial\alpha/\partial T)_{P;T=0} = -\gamma'(P)/V(0,P) < 0$ is plotted in Fig. 19 as a function of pressure. At low pressures, it increases upon increase of pressure, but decreases again for pressures $P \gtrsim 15$ bar. This surprising nonmonotonic behavior implies that the curves of α cross at very low temperatures.

At higher temperatures the expansion coefficient shows ''normal'' behavior with $\alpha > 0$, leading to a minimum in α vs T. Since $\alpha^2 \ll (\partial\alpha/\partial T)_P$ at low temperatures, the thermodynamic relation

$$\left(\frac{\partial C_P}{\partial P}\right)_T = -VT\left[\alpha^2 + \left(\frac{\partial\alpha}{\partial T}\right)_P\right] \tag{32}$$

implies $(\partial\alpha/\partial T)_P \approx -(1/VT)(\partial C_P/\partial P)_T = 0$ at $T_+ = 0.16$ K, i.e., the minima of α are essentially all located at T_+ where the specific-heat curves cross (see Figs. 16 and 17). The very weak pressure dependence of these minima is due to the small width of the crossing region of the specific-heat curves (see Fig. 5) as discussed above.

Our evaluation may be compared with earlier determinations of $\alpha(T,P)$. We find good agreement with the data of Abraham and Osborne;[15] for $P \gtrsim 1$ bar the differences are below 1.6×10^{-3} K^{-1} except for $0.1 \lesssim T \lesssim 0.4$ K, where

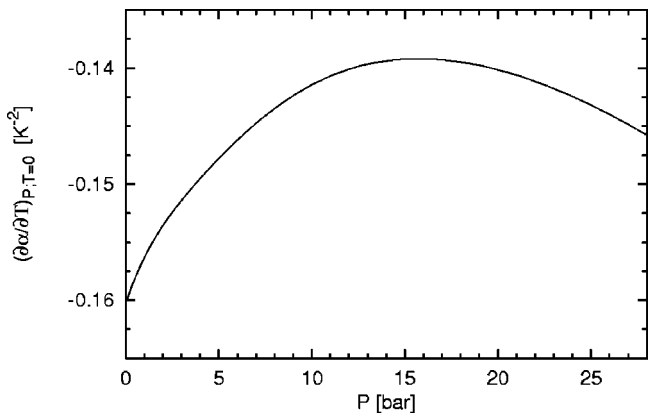

FIG. 19. Pressure dependence of the thermal expansion coefficient, $(\partial\alpha/\partial T)_P$, in the limit $T \to 0$.

they are as high as 10^{-2} K^{-1} due to different locations of the minima of $\alpha(T,P)$. Our data also agree with the data by Boghosian *et al.*[13] listed in Wilks' book[6] within 10^{-3} K^{-1} for $T<1$ K or $P>10$ bar, and 6×10^{-3} K^{-1} for $T\geqslant1$ K and $P\lesssim10$ bar. However, there are also qualitative differences, as we will now discuss.

In Fig. 17 the curves of $\alpha(T,P)$ are seen to cross near $T\approx0.35$ K in a rather broad range of temperatures, as was already observed by Lee *et al.*[11] By contrast, in some of the earlier measurements of $\alpha(T,P)$ a *sharp* crossing of these curves had been reported. For example, Brewer and Daunt[9] presented a figure with a sharp crossing point of the curves at $T=0.4$ K for pressures in the range from 2 to 22 bar, but noted that the sharpness of this feature could not be decided with certainty. In Wilks' book[6] $\alpha(T,P)$ is also plotted with a sharp crossing point at $T=0.35$ K for pressures 0–25 bar, although the error bars are of the order of 10^{-3} K^{-1}, i.e., are much larger than the suggested accuracy of the crossing point.

Our evaluation of the expansion coefficient clearly shows that the curves of $\alpha(T,P)$ do not cross at a single well-defined temperature. The condition for a crossing at some temperature $T'_+(P)$ is $(\partial\alpha/\partial P)_T=0$; for $P=10$ bar we have $T'_+\approx0.3$ K. From the crossing condition we can estimate the width of the crossing region as

$$T'_+(P)=T'_+(10\ \text{bar})+\left[\left(\frac{\partial\alpha}{\partial P}\right)_T\Big/\left(\frac{\partial^2\alpha}{\partial P\,\partial T}\right)\right]_{T'_+(10\ \text{bar})}. \tag{33}$$

In the pressure range $5\leqslant P\leqslant25$ bar the numerator of the second term on the right-hand side is of the order of 10^{-4} $K^{-1}\,bar^{-1}$, while the denominator is approximately 10^{-5} $K^{-2}\,bar^{-1}$. These values can be determined from Fig. 18 and Tables II–VIII, and are also consistent with the data of Refs. 6. Hence T'_+ varies by approximately 0.1 K over this pressure range, which is also consistent with the observed width of the crossing region in Fig. 17. This pressure dependence of T'_+ can also be recognized from Fig. 18 as the fact that $\alpha(T,P)$ never becomes a horizontal line as a function of P, contrary to the situation for the specific heat (Fig. 7). We conclude that for the curves of the expansion coefficient there exists only a broad crossing region, i.e., no sharp crossing point, in contrast to the data presented by Wilks.[6]

In summary, we showed that Greywall's[16] data contain the complete thermodynamic information for the normal-liquid phase of ^{3}He. This enabled us to calculate all equilibrium thermodynamic quantities for this phase at zero magnetic field for a wide range of parameters. We plotted and tabulated these data as reference material and benchmark for future investigations. In general, the published experimental data agree well with our evaluations. However the sharp crossing point of the curves of the expansion coefficient vs temperature for different pressures, summarized in Ref. 6, was found to be an artifact since it is not found in the thermodynamically consistent data presented here. The difference in the compressibility at low pressures ($P\lesssim2$ bar) between our values and the data obtained from Ref. 5 makes it highly desirable to have available high-precision data of the molar volume at a single temperature, which could be used in place of our Eq. (10). This would lead, in principle, to further improvements in the accuracy of the thermodynamic quantities calculated in this paper. The data of this paper may be calculated interactively for arbitrary input parameters on our website.[27]

Note added in proof. Recently, the experimental work by P. R. Roach *et al.*[28] came to our attention, where the isobaric expansion coefficient and the adiabatic compressibility were measured. Comparing their results for $P(T,V)-P(0,V)$ at three different temperatures with those obtained by Greywall,[16] the authors find a discrepancy of about 0.1 bar at $T=0.6$ K and high pressures which they attribute to Greywall's interpolation formulae, Eqs. (7)–(9).

*Present address: Dept. of Physics, Yale University, P.O. Box 208120, New Haven, CT 06520-8120.

[1] D. Pines and P. Nozières, *The Theory of Quantum Liquids* (Benjamin, New York, 1966).

[2] G. Baym and C. J. Pethick, in *The Physics of Liquid and Solid Helium*, Part II, edited by K. H. Bennemann and J. B. Ketterson (Wiley, New York, 1978), p. 1.

[3] D. M. Lee and R. Richardson, in *The Physics of Liquid and Solid Helium*, Part II (Ref. 2), p. 287.

[4] D. Vollhardt and P. Wölfle, *The Superfluid Phases of Helium 3* (Taylor and Francis, London, 1990).

[5] J. C. Wheatley, Rev. Mod. Phys. **47**, 415 (1975).

[6] J. Wilks, *The Properties of Liquid and Solid Helium* (Clarendon Press, Oxford, 1967).

[7] J. C. Wheatley, in *Progress in Low Temperature Physics*, edited by J. C. Gorter (North-Holland, Amsterdam, 1970), Vol. VI, p. 77.

[8] D. F. Brewer, J. G. Daunt, and A. K. Sreedhar, Phys. Rev. **115**, 836 (1959).

[9] D. F. Brewer and J. G. Daunt, Phys. Rev. **115**, 843 (1959).

[10] R. H. Sherman and F. J. Edeskuty, Ann. Phys. (N.Y.) **9**, 522 (1960).

[11] D. M. Lee, H. A. Fairbank, and E. J. Walker, Phys. Rev. **121**, 1258 (1961).

[12] E. C. Kerr and R. D. Taylor, Ann. Phys. (N.Y.) **20**, 450 (1962).

[13] C. Boghosian, H. Meyer, and J. E. Rives, Phys. Rev. **146**, 110 (1966).

[14] E. R. Grilly, J. Low Temp. Phys. **4**, 615 (1971).

[15] B. M. Abraham and D. W. Osborne, J. Low Temp. Phys. **5**, 345 (1971).

[16] D. Greywall, Phys. Rev. B **27**, 2747 (1983).

[17] In principle, one can use any sufficiently accurate set of data for the molar volume $V(T_0,P)$ at some fixed temperature T_0 for this purpose. However, since Greywall estimated his interpolation formula for $V(0.1\ K,P)$ to be accurate within 0.02 cm^3 (rms deviation) and used it to determine the volume of his experimental cell, we decided to employ his values of the molar volume, rather than other group's measurements of this quantity, thereby ensuring internal consistency.

[18] D. Greywall, Phys. Rev. B **31**, 2675 (1985).

[19] D. Greywall, Phys. Rev. B **33**, 7520 (1986).

[20] Greywall's interpolation formula $v_0(P)$ [Eq. (9)] is a fifth-order polynomial in P which parametrizes the data for the molar volume with sufficient accuracy (Ref. 17). However, the calculation

of the quantities $C_P - C_V$, $(\partial C_P/\partial P)_T$, $\kappa(T,P)$, and $\alpha(T,P)$ from $F(T,V)$ [Eq. (1)] involves also the derivative of $v_0(P)$, dv_0/dP. This is then only a fourth-order polynomial in P which is no longer sufficiently accurate. Therefore we reparametrized $v_0(P)$, or rather the inverse function $p_0(V)$ [Eq. (10)], by a polynomial of higher order.

[21] W. H. Press, S. A. Teukolsky, W. T. Vetterling, and B. P. Flannery, *Numerical Recipes in C* (Cambridge University Press, Cambridge, 1992).

[22] D. Greywall and P. A. Busch, J. Low Temp. Phys. **46**, 451 (1982).

[23] We note that the derivatives $(\partial V/\partial P)_{T_0}$ and $(\partial P/\partial V)_{T_0}$, obtained from Greywall's interpolation formula for $V(T_0,P)$ [Eq. (9)], cannot be expected to be as accurate as $V(T_0,P)$ itself. Since the variances of the coefficients in Eq. (9) are not known it is not possible to determine the accuracy of these derivatives with precision. However, the largest part of the problem was already removed by our reparametrization of $p_0(V)$ [Eq. (10)] (Ref. 20), which eliminates the shortcomings of fitting $V(T_0,P)$ by a rather low-order polynomial in P. The remaining systematic error in the derivative of the interpolation formula (9) will be largest at the two ends of the fit curve $v_0(P)$, i.e., at $P \lesssim 2$ bar and $P \gtrsim 27$ bar. Since $v_0(P)$ is most rapidly changing at small P we deduce that the error in $(\partial V/\partial P)_T$ is largest at $P \lesssim 2$ bar.

[24] In view of the unknown systematic error (Refs. 20 and 23) of $(\partial V/\partial P)_T$ and its implications for the compressibility especially at low pressures (see Sec. IV C), our values for $C_P(T,P=0)$, obtained from $C_P - C_V = VT\kappa(\partial P/\partial T)_V^2$ [Eq. (18)], may be subject to an error of at most a few percent at high temperatures.

[25] D. Vollhardt, Phys. Rev. Lett. **78**, 1307 (1997).

[26] Since α is proportional to κ [Eq. (20)] any inaccuracy in κ (see discussion above) will enter also in α.

[27] URL: http://www.physik.uni-augsburg.de/theo3/helium3/

[28] P. R. Roach *et al.*, J. Low Temp. Phys. **52**, 433 (1983).